# Cooperative upconversion as the gain-limiting factor in Er doped miniature Al$_2$O$_3$ optical waveguide amplifiers

P. G. Kik[a)] and A. Polman

*F.O.M. Institute for Atomic and Molecular Physics, P.O. Box 41883, 1009 DB Amsterdam, The Netherlands*

Erbium doped Al$_2$O$_3$ waveguide amplifiers were fabricated using two different doping methods, namely Er ion implantation into sputter deposited Al$_2$O$_3$, and co-sputtering from an Er$_2$O$_3$/Al$_2$O$_3$ target. Although the Er concentration in both materials is almost identical (0.28 and 0.31 at. %), the amplifiers show a completely different behavior. Upon pumping with 1.48 $\mu$m, the co-sputtered waveguide shows a strong green luminescence from the $^4S_{3/2}$ level, indicating efficient cooperative upconversion in this material. This is confirmed by pump power dependent measurements of the optical transmission at 1.53 $\mu$m and the spontaneous emission at 1.53 and 0.98 $\mu$m. All measurements can be accurately modeled using a set of rate equations that include first order and second order cooperative upconversion. The first order cooperative upconversion coefficient $C_{24}$ is found to be $3.5 \times 10^{-16}$ cm$^3$ s$^{-1}$ in the co-sputtered material, two orders of magnitude higher than the value obtained in Er implanted Al$_2$O$_3$ of $4.1 \times 10^{-18}$ cm$^3$ s$^{-1}$. It is concluded that the co-sputtering process results in a strongly inhomogeneous atomic scale spatial distribution of the Er ions. As a result, the co-sputtered waveguides do not show optical gain, while the implanted waveguides do. © *2003 American Institute of Physics.* [DOI: 10.1063/1.1565697]

## I. INTRODUCTION

Erbium doped waveguide amplifiers can be used in optical integrated circuits to compensate for signal losses by absorption, scattering, splitting, coupling, etc. Such waveguide amplifiers use stimulated emission from the first excited state ($^4I_{13/2}$) to the ground state ($^4I_{15/2}$) of Er$^{3+}$ at 1.53 $\mu$m [see Fig. 1(a)]. The intra-4$f$ transition is parity forbidden, and as a result the emission cross section is quite small ($\sim 10^{-21}$ cm$^2$). Consequently, high Er concentrations (0.1–1 at. %) are required to achieve significant amplification in waveguide structures on a cm length scale. At these high Er concentrations the closely spaced Er$^{3+}$ ions can interact. This causes several effects, such as energy migration,[1,2] in which an excited Er ion excites a neighboring unexcited Er ion (which may in turn be coupled to a nonradiative quenching site), and cooperative upconversion,[3–8] in which an excited Er ion promotes a neighboring excited Er ion into a higher lying state. Both processes are detrimental to the optical gain, as they reduce the population in the first excited state.

We compare the optical gain characteristics of two different optical waveguide amplifiers on silicon that have been fabricated either by Er$_2$O$_3$/Al$_2$O$_3$ co-sputtering or by Er ion implantation into Al$_2$O$_3$. We will show that although the Er concentrations in the two amplifiers are almost identical, the gain characteristics are entirely different, which is attributed to a difference in the atomic scale spatial distribution of the Er ions.

## II. EXPERIMENT

One waveguide structure was fabricated using radio-frequency Ar sputtering of a powder-pressed Er$_2$O$_3$/Al$_2$O$_3$ sputter target onto an oxidized Si substrate (SiO$_2$ thickness $\sim$5 $\mu$m). The target contained 2.8 wt. % Er$_2$O$_3$, corresponding to 0.31 at. % Er. The composition of the deposited film was measured by Rutherford backscattering spectrometry (RBS) using 2 MeV He$^+$ ions at a scattering angle of 165° (Fig. 2). The film thickness and the sample composition were determined from a fit to the data (solid line). The peak observed at channel $\sim$170 is related to the appearance of counts due to silicon atoms in the SiO$_2$ film beneath the Al$_2$O$_3$. The film thickness is found to be 570 nm, assuming an atomic density of $9.64 \times 10^{22}$ cm$^{-3}$. The Er concentration is constant over the full film thickness, and amounts to 0.31 at. %. The Al concentration is found to be 38 at. %, close to the stoichiometric composition of Al$_2$O$_3$. The film also contains a small amount of Ar (0.25 at. %) which is incorporated during the sputtering process. This material was annealed at 900 °C for 1 h in vacuum at a base pressure of $2 \times 10^{-7}$ mbar to optimize the Er luminescence intensity and lifetime.[9]

Ridge waveguides were formed in a 520-nm-thick layer using standard photolithography and Ar beam etching to a depth of 260 nm. The etch mask contained straight waveguides of $\sim$1 cm length, as well as a waveguide spiral geometry that confines a 3-cm-long waveguide on an area of 1 mm$^2$. Subsequently, a 1-$\mu$m-thick SiO$_2$ top cladding was deposited to reduce scattering losses. Figure 3 shows a scanning electron microscopy image of a 2-$\mu$m-wide Al$_2$O$_3$ ridge waveguide, after removal of the SiO$_2$ cladding layers. Before waveguide fabrication the Er photoluminescence (PL) lifetime at 1.535 $\mu$m in annealed co-sputtered films was found

---

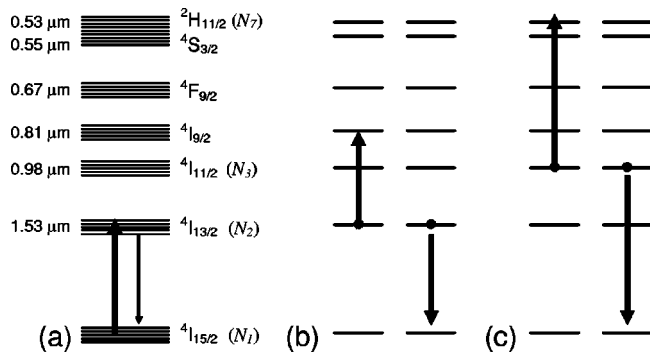a)Author to whom correspondence should be addressed: electronic mail: kik@caltech.edu

       5008       

FIG. 1. (a) Schematic representation of the Stark-split $Er^{3+}$ energy levels, showing excitation at 1.48 $\mu$m and emission at 1.53 $\mu$m. The energy levels are indexed using Russell–Saunders notation, and the corresponding populations $N_i$ are indicated. The emission wavelength due to radiative relaxation to the ground state is also included. (b) Cooperative upconversion from the $Er^{3+}$ first excited state, bringing one ion in the $^4I_{9/2}$ state. This is followed by rapid relaxation to the $^4I_{11/2}$ level, causing luminescence at 0.98 $\mu$m. (c) Cooperative upconversion from the $Er^{3+}$ second excited state, bringing one ion in the $^2H_{11/2}$ state that luminesces in the green.



FIG. 3. Scanning electron microscopy image of an Er doped $Al_2O_3$ ridge waveguide, fabricated by means of $Er_2O_3$ /$Al_2O_3$ co-sputtering. The $SiO_2$ cladding layers have been removed.

to be 6.2 ms. The waveguide fabrication reduces the lifetime to 1.7 ms, possibly due to the introduction of defects or impurities such as OH that are known to reduce the Er lifetime.

A second type of amplifier structure was fabricated by sputter deposition of a 600-nm-thick layer of $Al_2O_3$ from a pure $Al_2O_3$ sputter target, followed by Er ion implantation. An almost constant Er concentration of 0.28 at. % was achieved from 25 to 450 nm below the $Al_2O_3$ surface using multiple implants at energies in the range 100 keV–1.5 MeV. Waveguides were fabricated by etching to a depth of 300 nm. This material was previously shown to exhibit a net optical gain of 2.3 dB at 1.53 $\mu$m in a 4-cm-long waveguide ampli-

fier, at a coupled pump power of only 9 mW.[10] A detailed characterization of the optical properties of this material can be found in Refs. 9, 11 and 12.

To compare the optical gain characteristics of the co-sputtered and ion implanted waveguides, all measurements on the two sample types were performed under identical conditions. The waveguides were pumped using a continuous wave fiber-coupled 1.49 $\mu$m laser diode with a maximum power of 60 mW in the fiber. The pump light was butt coupled to the waveguides using a single-mode tapered fiber. Optical images of the waveguides were taken using a charge coupled device camera in combination with an optical microscope. Photoluminescence (PL) measurements were done by collecting the spontaneous emission from the waveguides normal to the sample using a multimode fiber placed approximately 1 mm above the sample surface. The collected luminescence was sent to a 48 cm grating monochromator. PL measurements in the range 1.0–1.7 $\mu$m were done using a 600 g/mm grating blazed at 1200 nm and a liquid nitrogen cooled Ge detector, in combination with standard lock-in techniques. PL lifetime measurements at visible frequencies were done using a 1200 g/mm grating blazed at 500 nm and a TE cooled AgOCs photomultiplier tube in combination with a photon counting system. Optical gain measurements were performed by adding a low power 1.530 $\mu$m signal from a NewFocus 6262 external cavity tunable diode laser to the input fiber, and monitoring the transmitted signal power as a function of applied pump power using a lock-in technique. The signal power in the input fiber was kept below 0.1 mW. The transmitted signal was collected by imaging the waveguide end facet onto a multimode fiber using a 40$\times$ microscope objective, and detected as in the PL measurements. A bandpass filter in the range 1.51–1.56 $\mu$m was placed in front of the monochromator entrance slit in order to suppress any pump related background signal.
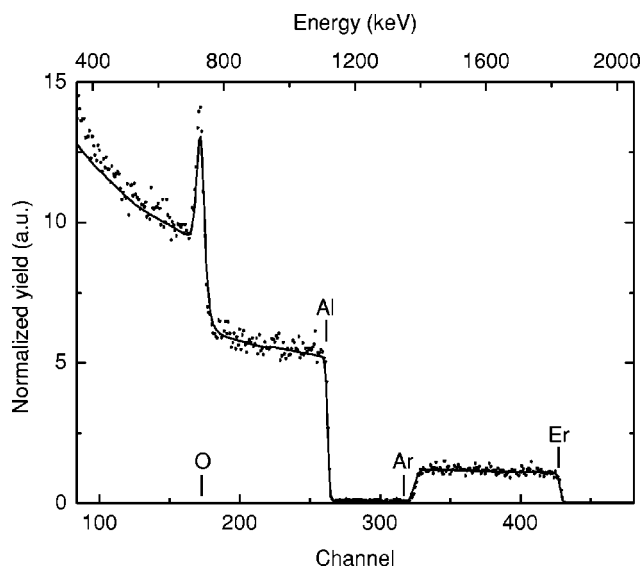


FIG. 2. Rutherford backscattering spectrometry measurement at a scattering angle of 165° of a 570-nm-thick Er doped $Al_2O_3$ film on $SiO_2$ made by $Er_2O_3$ /$Al_2O_3$ co-sputtering. The surface channels of the various elements are indicated. The solid line represents a fit assuming a constant Er concentration of 0.31 at. % over the full film thickness. The peak around channel 170 is the result of overlapping signals from aluminum in the top $Al_2O_3$ layer and silicon in the lower $SiO_2$ layer.
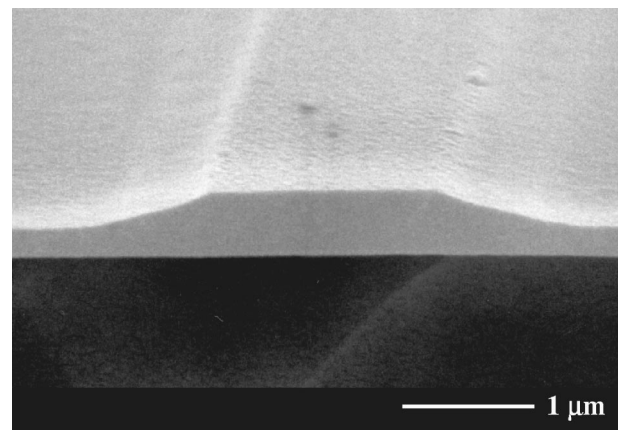
## III. RESULTS AND DISCUSSION

Figure 4(a) shows an optical image of an Er implanted $Al_2O_3$ spiral waveguide. The waveguide is pumped at 1.49 $\mu$m at a power of 60 mW in the input fiber. At this pump
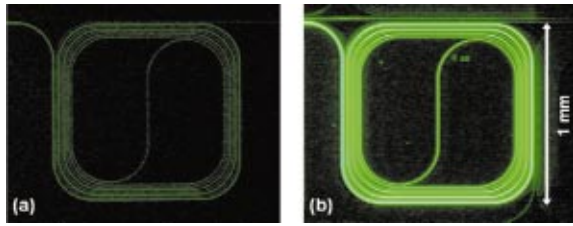
FIG. 4. (Color) (a) Optical image of a spiral waveguide amplifier doped with 0.28 at. % Er using ion implantation into $Al_2O_3$. The waveguide is pumped at 1.49 $\mu$m at a pump power of 60 mW in the input fiber. The waveguide emits green light as a result of two subsequent cooperative up-conversion interactions. (b) Optical image of a similar waveguide doped with 0.31 at. % Er using $Er_2O_3/Al_2O_3$ co-sputtering. The intense upconversion luminescence is ascribed to a strongly inhomogeneous atomic scale Er distribution.



FIG. 5. Measured transmission change at 1.53 $\mu$m as a function of 1.49 $\mu$m pump power in a 1-cm-long Er doped $Al_2O_3$ waveguide made by ion implantation (●) and in a 0.8-cm- long Er doped $Al_2O_3$ waveguide made by $Er_2O_3/Al_2O_3$ co-sputtering (○). The drawn lines are based on population calculations using the parameters in Table I. The $Er_2O_3/Al_2O_3$ co-sputtered waveguide shows a lower signal change due to strong cooperative upconversion.

power the waveguide can be seen to emit a faint green luminescence. Photoluminescence spectroscopy measurements of the visible emission (not shown) indicate that the green emission originates from the $^2H_{11/2}$ and $^4S_{3/2}$ levels of $Er^{3+}$. The luminescence seen in Fig. 4 also contains red emission from the $^4F_{9/2}$ level at 670 nm. These higher lying levels are populated via a two-step cooperative upconversion process, as depicted in Figs. 1(b) and 1(c). First, two Er ions in the $^4I_{13/2}$ state interact to yield an ion in the $^4I_{9/2}$ state [Fig. 1(b)], which is followed by a nonradiative relaxation to the $^4I_{11/2}$ level. Second, two ions in the $^4I_{11/2}$ level interact to yield an ion in the $^2H_{11/2}$ level [Fig. 1(c)], which relaxes to the $^4S_{3/2}$ level. Figure 4(b) shows an image of the $Er_2O_3/Al_2O_3$ co-sputtered waveguide taken under the same pumping conditions. This waveguide shows a very intense upconversion luminescence, even though the Er concentration is only slightly higher than in the ion implanted sample (0.31 vs 0.28 at. %).

The amount of optically active $Er^{3+}$ in the co-sputtered waveguide was determined from transmission measurements in the range 1.4–1.7 $\mu$m (not shown). The Er related peak absorption in the co-sputtered waveguide was found to be 3.1 dB/cm. Using the calculated overlap $\Gamma$ of the optical mode with the Er depth profile ($\Gamma = 49\%$), and the Er peak absorption cross section $\sigma_{12}^s$ of $5.8 \times 10^{-21}$ cm$^2$ taken from Ref. 11, the concentration of optically active Er in the waveguide is found to be $2.5 \times 10^{20}$ cm$^{-3}$, 17% less than the total Er concentration determined by RBS. This suggests that 83% of the Er is in the optically active 3+ valence state. The Er related peak absorption in the ion implanted waveguide is only 2.5 dB/cm, due to the lower mode overlap with the (shallower) Er implantation profile.

Figure 5 shows the measured signal transmission change at 1.530 $\mu$m as a function of applied pump power at 1.49 $\mu$m for a 1-cm-long straight waveguide made by ion implantation, and a 0.8-cm-long straight waveguide made by co-sputtering. A maximum signal transmission change of 2.5 dB is observed in the Er implanted waveguide, corresponding to the onset of Er related gain. Indeed, net optical gain was observed in this waveguide under slightly more optimized pumping conditions.[9] At the same pump power, the signal transmission in the co-sputtered waveguide has changed by only 1.2 dB, and consequently no Er related gain is obtained.
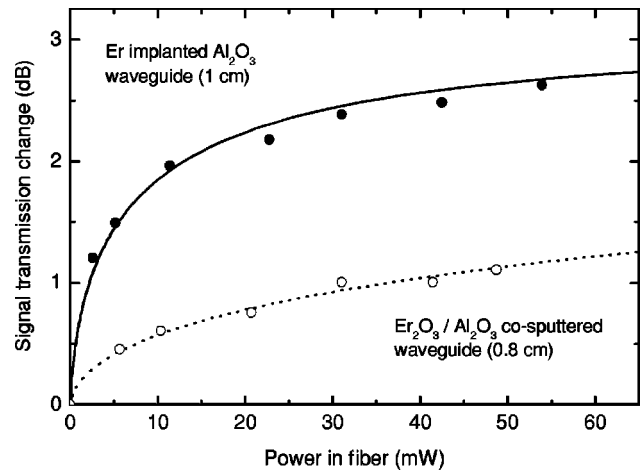
Note that the shape of the two curves in Fig. 5 is quite different, the ion implanted waveguide showing a stronger curvature. This is a consequence of the strong upconversion in the co-sputtered sample, as will be shown below.

To investigate the upconversion in the waveguides quantitatively, we have measured the spontaneous emission at 1.53 and 0.98 $\mu$m normal to the waveguide as a function of pump power. The luminescence was collected from the middle of the sample to avoid collection of pump light scattered from the input and output facets. The luminescence intensities found in both sample types are plotted in Fig. 6. At low pump power, the 1.53 $\mu$m luminescence from the ion implanted waveguide (solid squares) increases linearly with pump power. At pump powers above 1 mW in the fiber the intensity in both samples starts to show significant saturation, as was observed before.[12] An entirely different pump power dependence is seen in the co-sputtered waveguide. Within
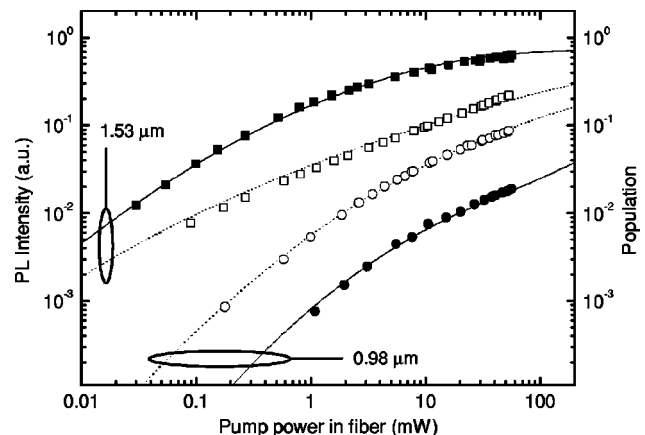


FIG. 6. Photoluminescence from Er doped $Al_2O_3$ waveguides pumped at 1.49 $\mu$m. Solid symbols refer to ion implanted material, open symbols to $Er_2O_3/Al_2O_3$ co-sputtered material. The drawn lines are calculations of the fraction of excited $Er^{3+}$ obtained using the parameters listed in Table I. The right axis indicates the corresponding fraction of excited Er.

the full range of applied pump powers, the 1.53 $\mu$m luminescence exhibits an almost perfect square-root dependence on pump power. Furthermore, the maximum 1.53 $\mu$m luminescence intensity in the co-sputtered waveguide is found to be significantly lower than in the ion implanted waveguide. This is consistent with the gain measurements in Fig. 5, which showed that the maximum achieved signal transmission change in the co-sputtered waveguide is lower than in the ion implanted waveguide. Figure 6 also shows the pump power dependence of the 0.98 $\mu$m luminescence from the $^4I_{11/2}$ state for the implanted (closed circles) and co-sputtered (open circles) waveguide. While the relative power dependence is similar, the co-sputtered waveguide shows a much higher luminescence intensity at 0.98 $\mu$m. This clearly shows that the co-sputtered sample exhibits stronger upconversion than the ion implanted sample. These findings are consistent with the intense green luminescence emitted by the co-sputtered waveguide [Fig. 4(b)], which is the result of upconversion from Er ions that are in the $^4I_{11/2}$ state.

In order to analyze the data in Figs. 5 and 6, we model the Er$^{3+}$ as a three-level system. This generally yields good results for the populations in the lower lying levels, because the population buildup in the levels above the $^4I_{11/2}$ level is small as a result of their low ($<1$ $\mu$s) lifetimes.[13] The short lifetime was confirmed for the $^2H_{11/2}$ and $^4S_{3/2}$ green emitting states, both of which showed a decay time of $<25$ $\mu$s limited by the time resolution of our system. The rate equations that determine the Er populations are

$$\frac{dN_3}{dt} = -(W_3 + C_{37}N_3)N_3 + (R_{24} + C_{24}N_2)N_2, \tag{1}$$

$$\frac{dN_2}{dt} = -(W_2 + R_{24} + R_{21} + 2C_{24}N_2)N_2 + W_3N_3$$
$$+ R_{12}N_1, \tag{2}$$

$$\frac{dN_1}{dt} = +(W_2 + R_{21} + C_{24}N_2)N_2 - R_{12}N_1 + C_{37}N_3 \tag{3}$$

with $N_i$ (cm$^{-3}$) the concentration of Er in level $i$ [see Fig. 1(a), $W_i = \tau_i^{-1}$ (s$^{-1}$) the measured spontaneous decay rate from level $i$, $R_{ij}$ (s$^{-1}$) a pump induced transition from level $i$ to level $j$, and $C_{ij}$ (cm$^3$ s$^{-1}$) the cooperative upconversion coefficient from level $i$, producing one ion in the ground state and one ion in level $j$. We have assumed that spontaneous decay from level 3 is dominated by nonradiative relaxation to level 2. The pump rates $R_{ij}$ are related to the photon flux $\varphi$ (cm$^{-2}$ s$^{-1}$) in the waveguide and the cross section $\sigma_{ij}^p$ (cm$^2$) for a pump induced transition from $i \rightarrow j$ according to $R_{ij} = \sigma_{ij}^p \times \varphi$. Note that stimulated emission and excited state absorption by the pump are included. The mean photon flux $\varphi$ is given by $\varphi = \eta \times P_{\text{fib}}/(E_{\text{phot}} \times A)$ with $\eta$ the coupling efficiency between the fiber and the waveguide, $P_{\text{fib}}$ (W) the power in the input fiber, $E_{\text{phot}}$ (J) the photon energy, and $A$ (cm$^2$) the effective optical mode area. The sum of all populations is equal to $N_0$, the concentration of optically active Er in the waveguide. Note that an Er ion excited to the $N_7$ level by second order upconversion from the $N_3$ level is assumed to relax back to the $N_3$ state immediately via multi-

phonon emission, and hence a single $C_{37}$ term appears in Eq. (1) [compared to a $2C_{24}N_2$ term in Eq. (2)]. The solutions of Eqs. (1)–(3) can be used to calculate the Er related signal change $G$ at 1.530 $\mu$m according to

$$G(\text{dB/cm}) = 10 \times {}^{10}\log(e) \times (\sigma_{21}^s N_2 - \sigma_{12}^s N_1 - \sigma_{24}^s N_2)$$
$$\times f_{\text{Er3+}} \times \Gamma, \tag{4}$$

with $\sigma_{ij}^s$ the cross section for a signal induced transition $i \rightarrow j$, $f_{\text{Er3+}}$ the fraction of Er in the optically active 3+ state, and $\Gamma$ the overlap of the optical mode with the Er doped core of the waveguide.

The rate Eqs. (1)–(3) were first solved analytically for steady state using the parameters as determined for ion implanted Al$_2$O$_3$ from Refs. 11 and 12. Upconversion from the second excited state (coefficient $C_{37}$) is assumed to be negligible in this case, since the green upconversion luminescence is very faint. The measured 1.53 and 0.98 $\mu$m PL intensities for the ion implanted waveguides were then multiplied by a scaling factor to match the fitted populations $N_2$ and $N_3$; while the coupling efficiency ($\eta$) was used as a fitting parameter for the power scale. Optimum agreement between the calculations and the measurements for the implanted sample is obtained for $\eta = 0.03$. Using these parameters, the 1.53 $\mu$m luminescence is described very well. The 0.98 $\mu$m luminescence at high power, however, is overestimated, suggesting that the used cross section for excited state absorption (taken from Ref. 11) is too high for this sample. A good fit is obtained using $\sigma_{24}^p = 0.25 \times 10^{-21}$ cm$^2$. Using these parameters the gain measurement for the ion implanted sample can be fitted assuming an optically active Er fraction of 83%. All parameters used are summarized in Table I. The calculations for the implanted sample are included in Figs. 5 and 6 (drawn lines). The three experimental data sets in Figs. 5 and 6 are reproduced for all applied pump powers.

A similar analysis was done for the co-sputtered waveguide. The luminescence intensity curves in Fig. 6 were calculated using the cross sections found for the ion implanted sample and the luminescence lifetimes $\tau_2$ and $\tau_3$ as measured in the co-sputtered waveguide (see Table I). The upconversion coefficients $C_{24}$ and $C_{37}$, and the coupling efficiency $\eta$ were used as fit parameters. Using the values listed in Table I, the experimental data are reproduced quite well. In order to achieve the square root-like behavior over the full range of pump powers, a high upconversion coefficient $C_{24}$ of $3.5 \times 10^{-16}$ cm$^3$/s is required. The square root-like behavior can be understood as follows: in case of strong upconversion, the population in the first excited state will remain low at most applied pump powers, and the Er decay rate will be dominated by the term $2C_{24}N_2$ in Eq. (2). In the low population limit, we have $N_2 \propto R_{12}\tau_2 \approx R_{12}/(2C_{24}N_2)$. This gives $N_2 \propto (R_{12})^{1/2}$, which indeed produces the observed square root-like dependence of $N_2$ on pump power.

The upconversion coefficient $C_{24}$ found for the co-sputtered sample ($3.5 \times 10^{-16}$ cm$^3$ s$^{-1}$) is two orders of magnitude higher than the value measured in ion implanted waveguides ($4.1 \times 10^{-18}$ cm$^3$ s$^{-1}$). This strong Er–Er interaction at low Er concentration suggests that the Er in the co-sputtered material is not distributed homogeneously. Re-

TABLE I. Parameter values used in the gain calculations in Fig. 5 and the calculations of the pump power dependent photoluminescence intensities in Fig. 6. Values marked by * were obtained using the fitting procedure described in this article. The remaining values relating to the ion implanted sample were taken from Ref. 10.

| Parameter | Ion implanted | Co-sputtered |
|---|---|---|
| $C_{Er}$ (cm$^{-3}$) | $2.7 \times 10^{20}$ | $3.0 \times 10^{20}$ |
| $f_{Er3+}$ (%) | 83* | 83* |
| $\tau_2$ (ms) | 7.8 | 1.7 |
| $\tau_3$ ($\mu$s) | 30 | 55 |
| $C_{24}$ (cm$^3$ s$^{-1}$) | $4.1 \times 10^{-18}$ | $3.5 \times 10^{-16*}$ |
| $C_{37}$ (cm$^3$ s$^{-1}$) | ⋯ | $8 \times 10^{-16*}$ |
| $\sigma_{12}^p$ (cm$^2$) | $2.7 \times 10^{-21}$ | id. |
| $\sigma_{21}^p$ (cm$^2$) | $0.77 \times 10^{-21}$ | id. |
| $\sigma_{24}^p$ (cm$^2$) | $0.25 \times 10^{-21*}$ | id. |
| $\sigma_{12}^s$ (cm$^2$) | $5.8 \times 10^{-21}$ | id. |
| $\sigma_{21}^s$ (cm$^2$) | $6.1 \times 10^{-21}$ | id. |
| $\sigma_{24}^s$ (cm$^2$) | $0.25 \times 10^{-21*}$ | id. |
| $L$ (cm) | 1 | 0.8 |
| $\eta$ (%) | 3* | 7* |
| $\Gamma$ (%) | 36* | 49* |

gions with a high local Er concentration could form in different ways. The use of an $Er_2O_3/Al_2O_3$ powder-mixed sputter target could, for example, result in the deposition of $Er_2O_3$ molecules, which yields a small Er–Er separation at low average Er concentration. Alternatively, during sputter deposition the Er ions may migrate over the sample surface, and form regions of high Er concentration. Such mechanism would be favored by the large difference in ionic radius of $Al^{3+}$ and $Er^{3+}$ (0.68 and 1.03 Å, respectively), making incorporation of an Er ion onto an Al lattice site unlikely.

To distinguish between the presence of ''molecular'' aggregates or more extended regions with high Er concentration we performed ion beam mixing experiments, in which a co-sputtered film was irradiated with 2 MeV Xe ions to a fluence of $2.5 \times 10^{15}$ cm$^{-2}$. Under these conditions each atom in the film will be displaced >5 times, as was calculated using the Monte Carlo simulation program TRIM. If the high upconversion coefficient is caused by the presence of separate $Er_2O_3$ molecules, the ion beam mixing should substantially reduce $C_{24}$. However, no influence of ion beam mixing on the gain characteristics or the pump power dependent luminescence was observed. It is therefore more likely that the co-sputtered film contains more extensive regions of relatively high Er concentration, possibly resulting from diffusion during the sputtering process. We have performed high-resolution transmission electron microscopy and x-ray diffraction measurements to search for regions of high Er content but found no evidence for these within the resolution of these techniques. Techniques more sensitive to the local atomic environment of the Er ions, such as extended x-ray absorption fine structure spectroscopy or high-resolution electron microscopy in combination with energy loss spectroscopy may resolve this issue.

The success of ion implantation in this comparison lies in the nonequilibrium nature of the implantation process, allowing for a relatively homogeneous Er distribution. For commercial applications of miniature optical amplifiers, different growth methods and different materials compositions should be further investigated. A low upconversion coefficient may, for example, be obtained by increasing the Er solubility by varying the waveguide composition. Alternatively, depositing at low temperature or at a high deposition rate will minimize effects such as diffusion, and may also reduce the effect of upconversion.

## IV. CONCLUSIONS

We have fabricated two types of miniature optical waveguide amplifiers, by Er ion implantation into $Al_2O_3$, and by $Er_2O_3/Al_2O_3$ co-sputtering. It is found that the cooperative upconversion coefficient $C_{24}$ in the co-sputtered material is two orders of magnitude higher than in the ion implanted material. As a result the co-sputtered material shows no optical gain, while the implanted material does. The high upconversion coefficient is attributed to a strongly nonhomogeneous Er distribution resulting from the co-sputtering process.

[1] F. Auzel, *Radiationless Processes*, edited by B. DiBartolo (Plenum, New York, 1980).
[2] E. Snoeks, P. G. Kik, and A. Polman, Opt. Mater. **5**, 159 (1996).
[3] W. J. Miniscalco, J. Lightwave Technol. **9**, 234 (1991).
[4] P. Blixt, J. Nilsson, T. Carlnäs, and B. Jaskorzynska, IEEE Photonics Technol. Lett. **3**, 996 (1991).
[5] F. Horst, T. H. Hoekstra, P. V. Lambeck, and T. J. A. Popma, Opt. Quantum Electron. **26**, S285 (1994).
[6] F. Dipasquale and M. Federighi, J. Lightwave Technol. **13**, 1858 (1995).
[7] T. Ohtsuki, S. Honkanen, S. I. Najafi, and N. Peyghambarian, J. Opt. Soc. Am. B **14**, 1838 (1997).
[8] B. C. Hwang, S. B. Jiang, T. Luo, J. Watson, G. Sorbello, and N. Peyghambarian, J. Opt. Soc. Am. B **17**, 833 (2000).
[9] G. N. van den Hoven, E. Snoeks, A. Polman, J. W. M. van Uffelen, Y. S. Oei, and M. K. Smit, Appl. Phys. Lett. **62**, 3065 (1993).
[10] G. N. van den Hoven, R. J. I. M. Koper, A. Polman, C. van Dam, J. W. M. van Uffelen, and M. K. Smit, Appl. Phys. Lett. **68**, 1886 (1996).
[11] G. N. van den Hoven, J. A. van der Elsken, A. Polman, C. van Dam, J. W. M. van Uffelen, and M. K. Smit, Appl. Opt. **36**, 3338 (1997).
[12] G. N. van den Hoven, E. Snoeks, A. Polman, C. van Dam, J. W. M. van Uffelen, and M. K. Smit, J. Appl. Phys. **79**, 1258 (1996).
[13] See, e.g., E. Desurvire, *Erbium-Doped Fiber Amplifiers* (Wiley, New York, 1994).